NRL Release Number 05-1226-2239

Analytical Approach to Calculation of Probability of Bit Error and Optimum Thresholds in Free-Space Optical Communication

Nader Namazi[a1], Ray Burris[b], G. Charmaine Gilbreath[c]

[a]Department of Electrical Engineering and Computer Science,
The Catholic University of America, Washington, DC 20064;
[b]Research Support Instruments, Inc., Lanham, MD 20706;
[c]Naval Research Laboratory, Washington, DC 20375

ABSTRACT

Based on the wavelet transformation and adaptive Wiener Filtering, a new method was presented by the authors to perform the synchronization and detection of the binary data from the Free-Space Optical (FSO) signal [1]. It was shown in [1] that the Haar wavelet with a fixed scale is an excellent choice for this purpose. The output of the filter is zero-mean and is closely related to the derivative of the binary data. In this effort an analysis of the work in [1] is presented to obtain the probability of bit error using a Bayesian ternary hypotheses testing. The analysis also results in determining optimum thresholds for the detection of binary data.

Keywords: free-space optical communication, detection, wavelet transformation, Haar wavelet, ternary hypotheses, optimum thresholding, bit error

1. INTRODUCTION

Free-Space Optical (FSO) communication system is an important area of research due to its important advantages of providing a very large bandwidth and relatively low cost of implementation. These systems have many desirable applications, perhaps the most important of which is their use in providing connection from the high bandwidth fiber-optic backbone to the buildings and businesses desiring high bandwidth access without the high cost of installing fiber through the local infrastructure. The FSO communication systems also have numerous advantages over the Free-Space RF (FSRF) systems.

Bit rates of FSO systems are approaching 100 Gbits/sec [2-5]. Besides, atmospheric propagation effects cause the FSO channel to be 'bursty' in nature and highly variable with a rate of change as high as 1 kHz and with power fades greater than 10 dB. Therefore, because of a very high bit rate and a time-varying channel, the bit error reduction is a difficult and vital area of research. The purpose of this paper is to introduce and implement a new and effective method to deal with these issues.

[1] namazi@cua.edu; phone 1 202 319-6153; fax 1 202 319-5195

Free-Space Laser Communications V, edited by David G. Voelz, Jennifer C. Ricklin, Proc. of SPIE Vol. 5892
(SPIE, Bellingham, WA, 2005) · 0277-786X/05/$15 · doi: 10.1117/12.619236

In a typical RF digital communication problem, the binary data is designed to avoid Inter-symbol Interference (ISI) and is digitally modulated. Here, the channel is, in general, modeled as band-limited, Additive, White and Gaussian Noise (AWGN), and the demodulated data consists of a string of pulses with a constant power. The value of the mean is typically zero and the variance of the data is a constant. The detection problem, therefore, is to use matched filtering and constant thresholding to identify the digital data. In contrast, the FSO communication channels can be modeled as wide-band and time-varying systems. The selected format of the binary data is typically NRZ-L[2] [6, p294], with no sinusoidal modulation. The received FSO signal consists of a high frequency data, which is varying in its amplitude. This corresponds to a non-stationary data with variable and irregular values of mean and variance. Consequently, the conventional matched filtering and constant thresholding is not applicable. Figure 1 displays a typical received FSO signal. This figure shows that the binary data is a noise-like signal with variable variance and mean. The data can be viewed as a high frequency signal modulating a relatively much lower frequency waveform. In this paper an analysis of the work in [1] is presented to obtain the probability of bit error using a Bayesian ternary hypotheses testing. The analysis also results in determining optimum thresholds for the detection of binary data.

2. MATHEMATICAL MODELING AND PROCESSING OF FSO SIGNAL

The received FSO data can be mathematically described as follows:

$$r(t) = \sigma(t)d(t) + m_L(t) + m_H(t) \qquad \textbf{(1)}$$

where $d(t)$ represents the binary data (message) and $\sigma(t)$ signifies the variation of the signal amplitude due to atmospheric transmission effects. In addition, the model assumes two types of additive noise. The first noise, $m_L(t)$, stands for the relatively low-frequency fluctuations of the signal mean value caused by insufficient ac coupling. The second term, $m_H(t)$, characterizes the additive white Gaussian noise (AWGN) with zero-mean. As reported by the authors in [1], and depicted in Figure 2, we first pass the data $r(t)$ through an adaptive Wiener Filter (AWF) for denoising. The output of this filter is then passed through a Haar Wavelet transformer with the transfer function [1]:

$$G(j\omega; a) = j\sqrt{|a|}\left\{\frac{\sin^2 \frac{a\omega}{4}}{\frac{a\omega}{4}}\right\} e^{ja\omega/2} \qquad \textbf{(2)}$$

[2] "One" is represented by level "+1" and "Zero" is represented by level "-1".

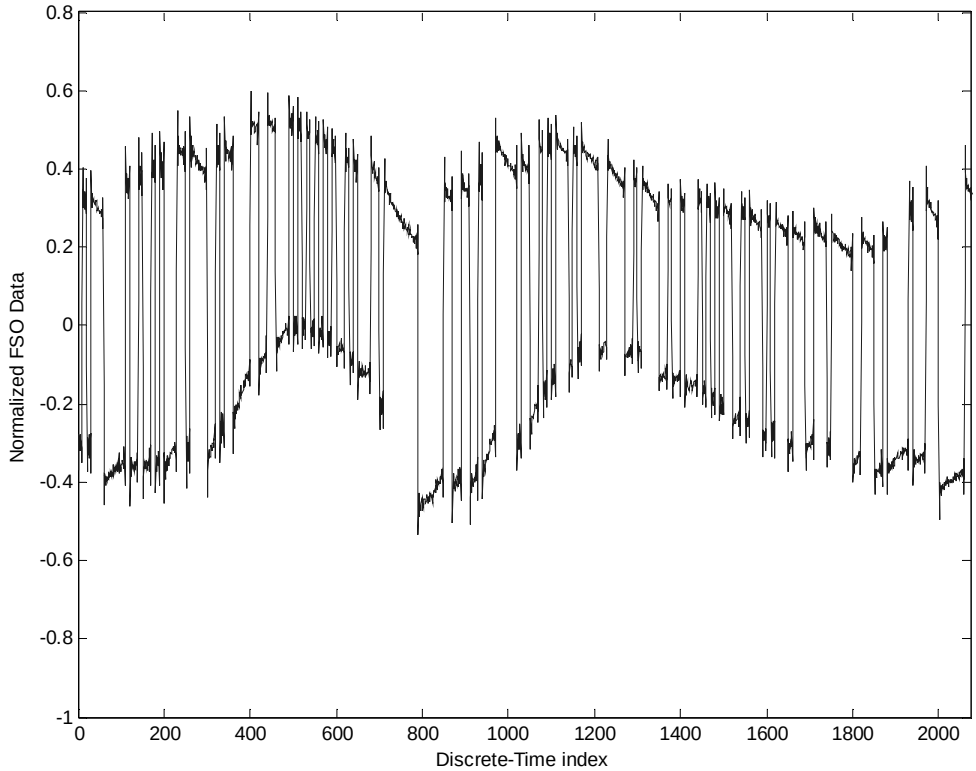

Figure 1. A Frame of Received FSO Data

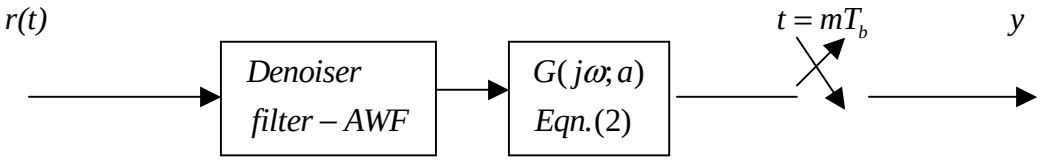

Figure 2. Filtering and Sampling of Received Data

where a is the scale of the Haar wavelet. Figure 3 depicts a typical FSO data at the input and the output of the filter (2) with fixed scale a. As shown in this figure, the filter, shown by (2), efficiently removes $m_L(t)$ in (1), and transforms the received data into a zero-mean signal resembling an approximation of its derivative. The filtered data, as depicted in Figure 3, is then sampled at the multiple integers of bit time, assuming that it has been properly synchronized [1]. In the following section, we establish a ternary hypotheses test to calculate the probability of bit error.

3. CALCULATION OF PROBABILITY OF BIT ERROR

This section is devoted to the calculation of the probability of bit error. In view of Figure 3, the output y of the sampler shown in Figure 2 can be considered as a scalar random variable, which can be characterized by a ternary hypotheses test as follows[3]:

$$\begin{aligned} H_0: &\quad y = w, \\ H_1: &\quad y = +d.f_1 + w, \\ H_2: &\quad y = -d.f_2 + w, \end{aligned} \qquad \textbf{(3)}$$

where (3) is followed from (1) assuming that the residual noise at the output of the sampler is characterized by w and is considered to be white and Gaussian with mean zero. In addition, f_i, $i = 1, 2$ are Rayleigh fading random variables, independent of w, and d represents a known, non-negative quantity proportional to energy of the binary data. Without loss of generality, we assume that $d = 1$. Hypothesis H_0 corresponds to a scenario for which, at the transition time, there has not been any bit change $(d = 0)$, and hypotheses H_1 and H_2, on the other hand, represent circumstances for which bit transitions have occurred from low-to-high and high-to-low, respectively. Based on the aforementioned assumptions, we can establish a ternary hypotheses test by determining the conditional probability density functions (pdf) of y given the three hypotheses H_0, H_1 and H_2 [7 P23]. A maximum likelihood detector can then be implemented by evaluating these pdf's at any given observation Y and select the largest.

[3] We use lower case letters for a random variable. Upper case letters are utilized to signify the running values of the corresponding random variable. Also, the model (3) considers the fact that the fading channel may act differently for high and low bits.

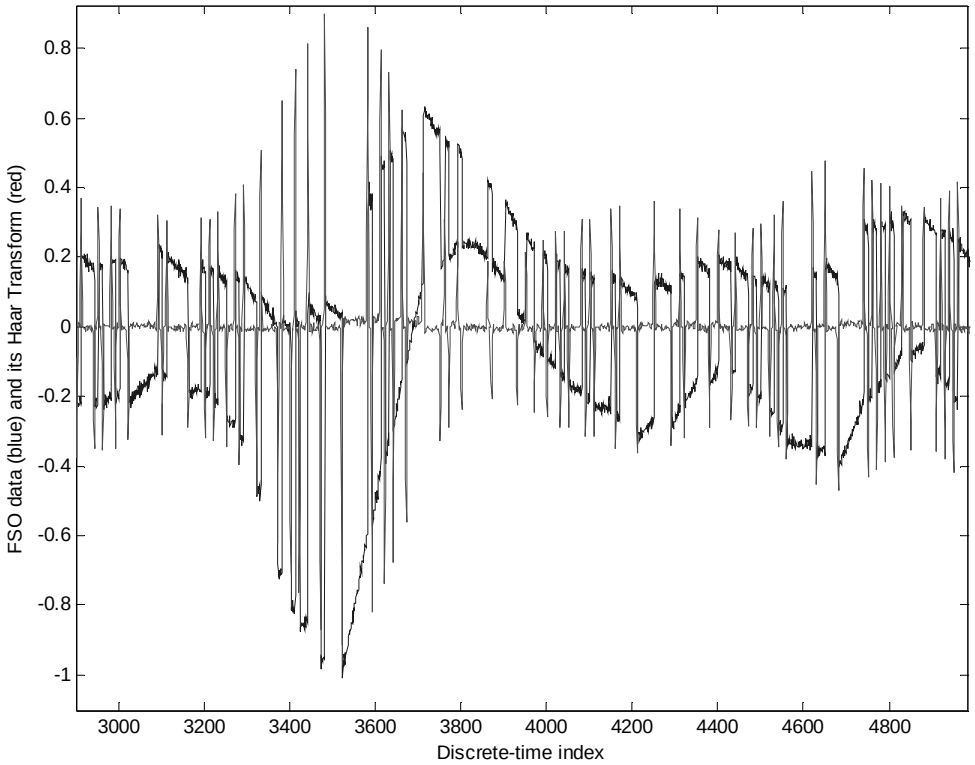

Figure 3. Portion of the FSO Data (blue) and its Corresponding CWT (red)

To begin, note that

$$p_y(Y \mid H_0) = \frac{1}{\sqrt{2\pi\sigma_w^2}} e^{-Y^2/2\sigma_w^2} \tag{4}$$

Accordingly,

$$p_y(Y \mid H_1, F_1) = \frac{1}{\sqrt{2\pi\sigma_w^2}} e^{-(Y-F_1)^2/2\sigma_w^2} \tag{5}$$

and

$$p_y(Y \mid H_2, F_2) = \frac{1}{\sqrt{2\pi\sigma_w^2}} e^{-(Y+F_2)^2/2\sigma_w^2} \tag{6}$$

Also, by definition, f_i, $i = 1, 2$ are Rayleigh distributed random variables; therefore,

$$p_f(F_i) = \frac{F_i}{\sigma_{f_i}^2} e^{-F_i^2/2\sigma_{f_i}^2} u(F_i) \tag{7}$$

where $u(.)$ is the step-function. It follows from (5) and (7) that

$$\begin{aligned} p_y(Y \mid H_1) &= \int_0^\infty \frac{1}{\sqrt{2\pi\sigma_w^2}} e^{-(Y-F_1)^2/2\sigma_w^2} p_{f_1}(F_1) dF_1 \\ &= \frac{1}{B_1\sigma_{f_1}^2} p_y(Y \mid H_0) \left\{ 1 + \frac{\sqrt{2\pi}}{\sqrt{B_1}\sigma_w^2} Y e^{Y^2/2B_1\sigma_w^4} Q\left(\frac{-Y}{\sqrt{B_1}\sigma_w^2}\right) \right\} \end{aligned} \tag{8}$$

where

$$B_1 = \frac{\sigma_w^2 + \sigma_{f_1}^2}{\sigma_w^2 \sigma_{f_1}^2} \tag{9}$$

and

$$Q(x) \triangleq \frac{1}{\sqrt{2\pi}} \int_x^\infty e^{-x^2/2} dx \tag{10-a}$$

with the known property that

$$Q(x)+Q(-x)=1 \qquad \textbf{(10-b)}$$

Similarly, it can be shown that

$$p_y(Y\mid H_2)=\frac{1}{B_2\sigma_{f_2}^2}\,p_y(Y\mid H_0)\left\{1-\frac{\sqrt{2\pi}}{\sqrt{B_2}\sigma_w^2}Ye^{Y^2/2B_2\sigma_w^4}Q(\frac{Y}{\sqrt{B_2}\sigma_w^2})\right\} \qquad \textbf{(11)}$$

wherein

$$B_2=\frac{\sigma_w^2+\sigma_{f_2}^2}{\sigma_w^2\sigma_{f_2}^2} \qquad \textbf{(12)}$$

It is noted that the value of Y for which $p_y(Y\mid H_1)=p_y(Y\mid H_0)$ characterizes the threshold value T_1. Similarly, the values of Y for which $p_y(Y\mid H_2)=p_y(Y\mid H_0)$ signifies the threshold value T_2. Consequently, it follows from (8) that at $Y=T_1$ we attain

$$\frac{1}{B_1\sigma_{f_1}^2}\left\{1+\frac{\sqrt{2\pi}}{\sqrt{B_1}\sigma_w^2}Ye^{Y^2/2B_1\sigma_w^4}Q(\frac{-Y}{\sqrt{B_1}\sigma_w^2})\right\}=1 \qquad \textbf{(13)}$$

Correspondingly, it follows from (11) that at $Y=T_2$ we obtain

$$\frac{1}{B_2\sigma_{f_2}^2}\left\{1-\frac{\sqrt{2\pi}}{\sqrt{B_2}\sigma_w^2}Ye^{Y^2/2B_2\sigma_w^4}Q(\frac{Y}{\sqrt{B_2}\sigma_w^2})\right\}=1 \qquad \textbf{(14)}$$

For convenience, define an auxiliary function $g_1(Z)$ as follows:

$$g_1(Z)=A_1\left\{1+\sqrt{2\pi}Ze^{Z^2/2}Q(-Z)\right\} \qquad \textbf{(15)}$$

where $A_1=\frac{1}{B_1\sigma_{f_1}^2}$ and $Z=\frac{Y}{\sqrt{B_1}\sigma_w^2}$. It follows from (15) that the value of $Z=\zeta$ for which $g_1(Z)=1$ can be used to determine the threshold value T_1; that is,

$$T_1=\sqrt{B_1}\sigma_w^2\zeta \qquad \textbf{(16)}$$

Note also from (9) and (16) that

$$T_1 = \left(\frac{\sigma_w^2 + \sigma_{f_1}^2}{\sigma_{f_1}^2} \right)^{1/2} \sigma_w \zeta. \qquad \textbf{(17)}$$

In view of (14), the threshold T_2 can be evaluated in a similar fashion. To demonstrate, let

$$g_2(Z) = A_2 \left\{ 1 - \sqrt{2\pi} Z e^{Z^2/2} Q(Z) \right\} \qquad \textbf{(18)}$$

where $A_2 = \dfrac{1}{B_2 \sigma_{f_2}^2}$ and $Z = \dfrac{Y}{\sqrt{B_2} \sigma_w^2}$. Then,

$$T_2 = \left(\frac{\sigma_w^2 + \sigma_{f_2}^2}{\sigma_{f_2}^2} \right)^{1/2} \sigma_w \psi \qquad \textbf{(19)}$$

in which ψ represents the value of Z for which $g_2(Z) = 1$.

Once T_1 and T_2 are calculated, we can obtain the average probability of error which can be obtained by considering the conditional probability of incorrect reception $P(\varepsilon \mid H_i)$ as

$$P(\varepsilon) = \frac{1}{3} \left[P(\varepsilon \mid H_0) + P(\varepsilon \mid H_1) + P(\varepsilon \mid H_2) \right] \qquad \textbf{(20)}$$

where, without loss of generality, it is assumed that the hypotheses are all equally likely. It follows from Figure (4), and (10-b), that

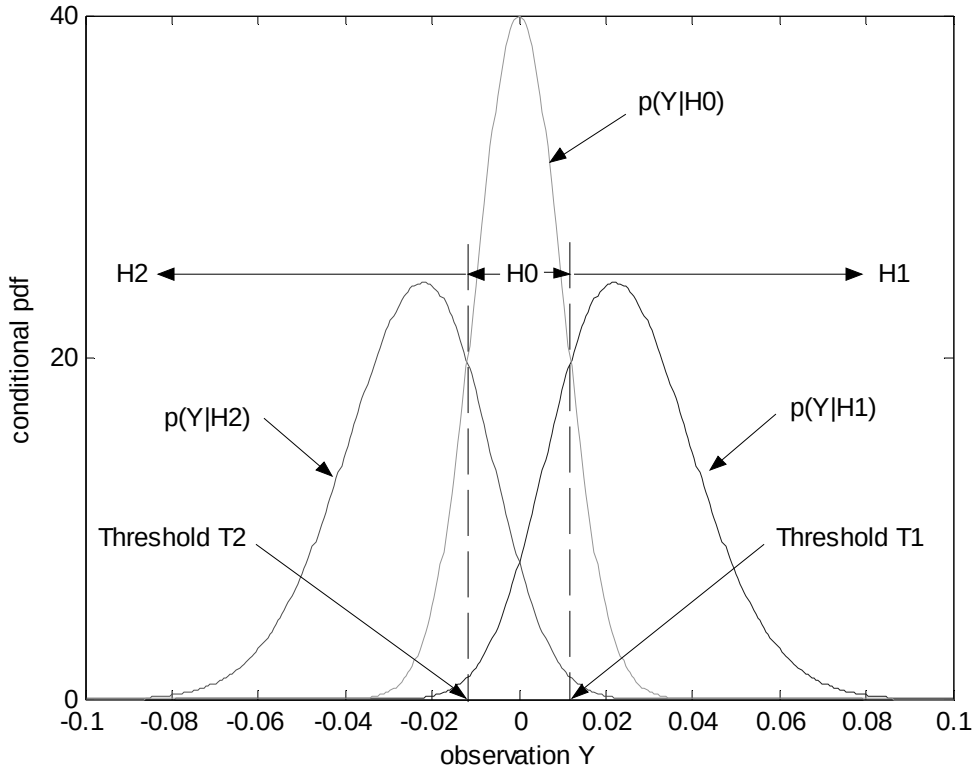

Figure 4. Conditional pdf's of the Ternary Hypotheses

$$P(\varepsilon \mid H_0) = 1 - \frac{1}{\sqrt{2\pi\sigma_w^2}} \int_{T_2}^{T_1} e^{-Y^2/2\sigma_w^2} dY = 1 - Q(T_2/\sigma_w) + Q(T_1/\sigma_w)$$
$$= Q(-T_2/\sigma_w) + Q(T_1/\sigma_w) \qquad \textbf{(21)}$$

Also, in view of Figure 4, it follows that

$$P(\varepsilon \mid H_1) = \int_{-\infty}^{T_1} p_y(Y \mid H_1) dY$$
$$= \int_{-\infty}^{T_1} \frac{1}{B_1 \sigma_{f_1}^2} p_y(Y \mid H_0) \left\{ 1 + \frac{\sqrt{2\pi}}{\sqrt{B_1}\sigma_w^2} Y e^{Y^2/2B_1\sigma_w^4} Q\left(\frac{-Y}{\sqrt{B_1}\sigma_w^2}\right) \right\} dY \qquad \textbf{(22)}$$

In Appendix A, it is shown that (22) becomes

$$P(\varepsilon \mid H_1) = \left[\frac{\sigma_w^2}{\sigma_w^2 + \sigma_{f_1}^2}\right]\left\{1 - Q\left[\left(\frac{\sigma_w^2 + \sigma_{f_1}^2}{\sigma_{f_1}^2}\right)^{1/2} \zeta\right]\right\} -$$
$$\left[\frac{\sigma_{f_1}^2}{\sigma_w^2 + \sigma_{f_1}^2}\right]^{1/2}\left\{e^{-\frac{1}{2}\left(\frac{\sigma_w^2}{\sigma_{f_1}^2}\right)\zeta^2}\left[1 - Q(\varsigma)\right] - \left[\frac{\sigma_{f_1}^2}{\sigma_w^2 + \sigma_{f_1}^2}\right]^{1/2}\left[1 - Q\left(\left[\frac{(\sigma_w^2 + \sigma_{f_1}^2)}{\sigma_{f_1}^2}\right]^{1/2} \zeta\right)\right]\right\}. \quad \textbf{(23)}$$

Using (10-b), (23) can be simplified as follows:

$$P(\varepsilon \mid H_1) = \left[\frac{1}{1 + \left(\sigma_{f_1}^2 / \sigma_w^2\right)}\right]\left\{Q\left[-\left(\frac{1 + \left(\sigma_{f_1}^2 / \sigma_w^2\right)}{\left(\sigma_{f_1}^2 / \sigma_w^2\right)}\right)^{1/2} \zeta\right]\right\} -$$
$$\left[\frac{\left(\sigma_{f_1}^2 / \sigma_w^2\right)}{1 + \left(\sigma_{f_1}^2 / \sigma_w^2\right)}\right]^{1/2}\left\{e^{-\frac{1}{2}\left(\frac{\sigma_w^2}{\sigma_{f_1}^2}\right)\zeta^2} Q(-\varsigma) - \left[\frac{\left(\sigma_{f_1}^2 / \sigma_w^2\right)}{1 + \left(\sigma_{f_1}^2 / \sigma_w^2\right)}\right]^{1/2} Q\left(-\left(\frac{1 + \left(\sigma_{f_1}^2 / \sigma_w^2\right)}{\left(\sigma_{f_1}^2 / \sigma_w^2\right)}\right)^{1/2} \zeta\right)\right\}. \quad \textbf{(24)}$$

It is noted from Figure 4 that

$$P(\varepsilon \mid H_2) = \int_{T_2}^{\infty} p_y(Y \mid H_2)dY = \int_{-\infty}^{-T_2} p_y(-Y \mid H_2)dY. \quad \textbf{(25)}$$

It is eminent from (8) and (11) that $p_y(-Y \mid H_2)$ and $p_y(Y \mid H_1)$ have the same forms when we replace B_1 with B_2, and $\sigma_{f_1}^2$ with $\sigma_{f_2}^2$. Hence, in view of (17), (19), and (25), $P(\varepsilon \mid H_2)$ can be realized from $P(\varepsilon \mid H_1)$, shown by (24), by switching B_1 to B_2, $\sigma_{f_1}^2$ to $\sigma_{f_2}^2$, and ς to $-\psi$; that is,

$$P(\varepsilon \mid H_2) = \left[\frac{1}{1 + \left(\sigma_{f2}^2 / \sigma_w^2\right)}\right]\left\{Q\left[\left(\frac{1 + \left(\sigma_{f2}^2 / \sigma_w^2\right)}{\left(\sigma_{f_2}^2 / \sigma_w^2\right)}\right)^{1/2} \psi\right]\right\} -$$
$$\left[\frac{\left(\sigma_{f_2}^2 / \sigma_w^2\right)}{1 + \left(\sigma_{f_2}^2 / \sigma_w^2\right)}\right]^{1/2}\left\{e^{-\frac{1}{2}\left(\frac{\sigma_w^2}{\sigma_{f_2}^2}\right)\psi^2} Q(\psi) - \left[\frac{\left(\sigma_{f2}^2 / \sigma_w^2\right)}{1 + \left(\sigma_{f_2}^2 / \sigma_w^2\right)}\right]^{1/2} Q\left(\left(\frac{1 + \left(\sigma_{f_2}^2 / \sigma_w^2\right)}{\left(\sigma_{f_2}^2 / \sigma_w^2\right)}\right)^{1/2} \psi\right)\right\}. \quad \textbf{(26)}$$

Hence, the total average probability of error can be calculated by substituting (21), (24) and (26) in (20). Finally, it should be mentioned that for the case for which $\sigma_{f_1}^2 = \sigma_{f_2}^2 = \sigma_f^2$, it follows that $B_1 = B_2$ and $T_1 = -T_2 = T$. Consequently, it is seen from (20) and (21) that $P(\varepsilon)$ becomes

$$P(\varepsilon) = \frac{2}{3}\left[Q(\frac{T}{\sigma_w}) + P(\varepsilon \mid H_1) \right]. \qquad \textbf{(27)}$$

In view of hypotheses H_1 and H_2 in (3), we define the *Distorted Signal-to-Noise Ratio (DSNR)* as:

$$DSNR_i = \frac{\sigma_d^2 \sigma_{f_i}^2}{\sigma_w^2}; \quad i = 1, 2. \qquad \textbf{(28)}$$

Since, by definition, $d = 1$, it follows from hypotheses H_1 and H_2 in (3) that $\sigma_d^2 = 1$. Consequently, from (28) we have

$$DSNR_i = \frac{\sigma_{f_i}^2}{\sigma_w^2}; \quad i = 1, 2. \qquad \textbf{(29)}$$

For convenience, we assume that $\sigma_{f_1}^2 = \sigma_{f_1}^2 = \sigma_f^2$; hence, $DSNR_1 = DSNR_2 = DSNR$. Figure 5 illustrates the total average probability of error (27) as a function of $DSNR$. This figure shows that as σ_f^2 / σ_w^2 increases, the probability of error decreases. Figure 6 depicts the normalized threshold T / σ_w as a function of σ_f^2 / σ_w^2. It is seen from this figure that the normalized threshold T / σ_w is a monotonic function of σ_f^2 / σ_w^2. A practical implication of this result is that the optimum threshold can be evaluated from Figure 6 by a table-look-up strategy. That is, once σ_f^2 / σ_w^2 is estimated, the normalized threshold is found from Figure 6, and the optimum threshold is estimated by multiplying the result by σ_w.

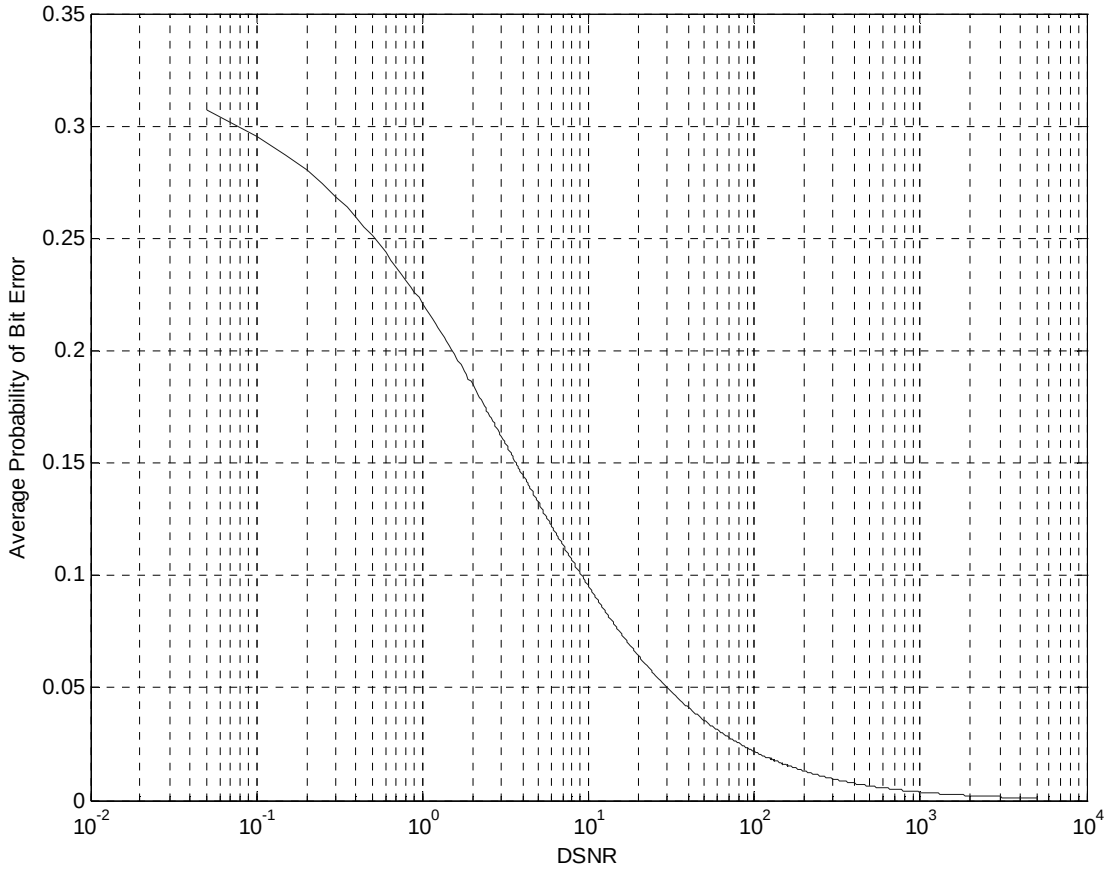

Figure 5. Average Probability of Bit Error Versus DSNR

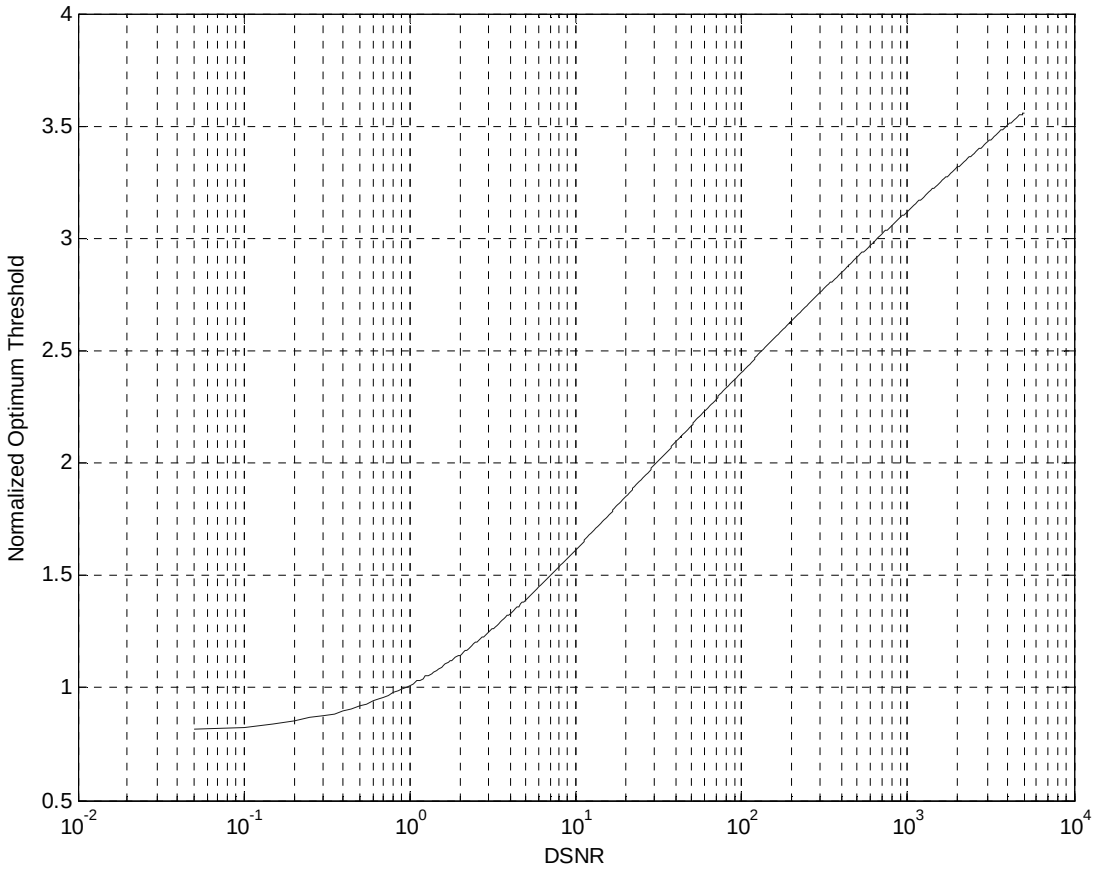

Figure 6. Normalized Optimum Threshold Versus DSNR

Appendix A – Derivation of $P(\varepsilon \mid H_1)$

The objective of this appendix is to illustrate the derivation of $P(\varepsilon \mid H_1)$ shown in (23). We know from (8) that

$$p_y(Y \mid H_1) = \frac{1}{B_1\sigma_{f_1}^2}\, p_y(Y \mid H_0)\left\{1 + \frac{\sqrt{2\pi}}{\sqrt{B_1}\sigma_w^2} Y e^{Y^2/2B_1\sigma_w^4} Q\left(\frac{-Y}{\sqrt{B_1}\sigma_w^2}\right)\right\} \qquad \textbf{(A-1)}$$

Hence, the conditional probability of error $P(\varepsilon \mid H_1)$ becomes

$$\begin{aligned} P(\varepsilon \mid H_1) &= \int_{-\infty}^{T_1} p_y(Y \mid H_1)dY = \frac{1}{B_1\sigma_{f_1}^2}\int_{-\infty}^{T_1} p_y(Y \mid H_0)dY \\ &+ \frac{\sqrt{2\pi}}{\sqrt{B_1}\sigma_w^2}\frac{1}{B_1\sigma_{f_1}^2}\int_{-\infty}^{T_1} p_y(Y \mid H_0) Y e^{Y^2/2B_1\sigma_w^4} Q\left(\frac{-Y}{\sqrt{B_1}\sigma_w^2}\right)dY. \end{aligned} \qquad \textbf{(A-2)}$$

Application of (4) in (A-2) renders,

$$P(\varepsilon \mid H_1) = \frac{1}{B_1\sigma_{f_1}^2}\left[1 - Q\left(\frac{T_1}{\sigma_w}\right)\right] + \kappa\int_{-\infty}^{T_1} e^{-\alpha^2 Y^2} Y dY - \kappa\int_{-\infty}^{T_1} e^{-\alpha^2 Y^2} Y Q(\beta Y) dY \qquad \textbf{(A-3)}$$

wherein

$$\begin{aligned} \alpha^2 &= \left[\frac{1}{2\sigma_w^2} - \frac{1}{2B_1\sigma_w^4}\right] \\ \kappa &= \frac{1}{B_1\sigma_{f_1}^2\sqrt{B_1}\sigma_w^3} \\ \beta &= \frac{1}{\sqrt{B_1}\sigma_w^2} \end{aligned} \qquad \textbf{(A-4)}$$

The last integral in (A-3) can be solved using integration by parts; that is,

$$\int u dv = uv - \int v du \qquad \textbf{(A-5)}$$

with

$$\begin{aligned} u &= Q(\beta Y) \\ dv &= e^{-\alpha^2 Y^2} Y dY. \end{aligned} \qquad \textbf{(A-6)}$$

Hence,

$$\int_{-\infty}^{T_1} e^{-\alpha^2 Y^2} Y Q(\beta Y) dY = \frac{-1}{2\alpha^2} Q(\beta T_1) e^{-\alpha^2 T_1^2} - \int_{-\infty}^{T_1} \frac{1}{2\alpha^2} e^{-\alpha^2 Y^2} e^{-\beta^2 Y^2} dY. \qquad \textbf{(A-7)}$$

Furthermore the second integral in (A-3) is solved as

$$\kappa \int_{-\infty}^{T_1} e^{-\alpha^2 Y^2} Y dY = -\frac{\kappa}{2\alpha^2} e^{-\alpha^2 T_1^2}. \qquad \textbf{(A-8)}$$

Applications of (17), (A-4), (A-7), and (A-8) in (A-3), after collection of terms and further simplification, finally leads to (23).

REFERENCES

1. N. Namazi, H. R. Burris, C. Conner, G. C. Gilbreath, W. Scharpf, “Synchronization and Detection of Binary Data in Free-Space Optical Communication Systems using Haar Wavelet Transformation”, SPIE Conference, August 2004.

2. H. R. Burris, C. Moore, M. Vilcheck, R. Mahon, M. Stell, M. Suite, M. Davis, W. Scharpf, A. Reed, W. Rabinovich, C. Gilbreath, E. Oh, N. M. Namazi, “Low Frequency Sampling Adaptive Thresholding for Free-Space Optical Communication Receivers with Multiplicative Noise”, SPIE Conference, July 2003.

3. H. Burris, A. Reed, N. Namazi, W. J. Scharpf, M. J. Vilcheck, M. F. Stell, M. R. Suite, "Adaptive Thresholding for Free-Space Optical Communication Receivers with Multiplicative Noise", 2002 IEEE Aerospace Conference at Big Sky, Montana, March 9-16, 2002.

4. H. Burris, A. Reed, N. Namazi, M. Vilcheck, M. Ferraro, "Use of Kalman Filtering in Optical Communication Systems with Multiplicative Noise", Proceedings of IEEE International Conference on Acoustics, Speech and Signal Processing (ICASSP'2001), Salt Lake City, Utah, May 2001.

5. G. C. Gilbreath, et al, “Large-Aperture multiple quantum well modulating retroreflector for free-space optical data transfer on unmanned aerial vehicles, Optical Engineering, 40(7) 1348-1356.

6. Ziemer Rodger E. and Peterson Roger L., *Digital Communications and Spread Spectrum Systems*, (Macmillan Publishing Company, Inc., 1985).

7. Van Trees Harry L., *Detection, Estimation, and Modulation Theory, Part I.*, (John Wiley and Sons, Inc., 1968).